PNAS RESEARCH ARTICLE | ASTRONOMY OPEN ACCESS

Spectroscopic Supermassive Dark Star candidates

Cosmin Ilie[a,1], Sayed Shafaat Mahmud[a], Jillian Paulin[b], and Katherine Freese[c,d,e,1]

Contributed by Katherine Freese; received June 2, 2025; accepted August 15, 2025; reviewed by Laura Baudis and Neelima Sehgal

Dark Stars (DSs), i.e., early stars composed almost entirely of hydrogen and helium but powered by Dark Matter (DM), could form in zero metallicity clouds located close to the center of high redshift DM halos. In 2023, three of us identified (in a PNAS work) the first three photometric DS candidates: JADES-GS-z11-0, JADES-GS-z12-0, and JADES-GS-z13-0. We report here our results of a follow-up analysis based on available NIRSpec JWST data. We find that JADES-GS-z11-0 and JADES-GS-z13-0 are spectroscopically consistent with a DS interpretation. Moreover, we find two additional spectroscopic DS candidates: JADES-GS-z14-0 and JADES-GS-z14-1, with the former being the second most distant luminous object ever observed. We furthermore identify, in the spectrum of JADES-GS-z14-0, a tentative feature ($S/N \sim 2$) indicative of the smoking gun signature of DSs: the He II λ1640 absorption line. In view of ALMA's recent identification of a probable O III nebular emission line in the spectrum of JADES-GS-z14-0, the simple interpretation of this object as an isolated DS is unlikely. If both spectral features survive follow-up observations, it would imply a DS embedded in a metal rich environment, requiring theoretical refinements of the formation of evolution of DSs, which in previous studies were assumed to form in isolation, without any companions.

stars | cosmology | Dark Matter | James Webb Space Telescope | high-z galaxies

Significance

In 2007 Spolyar, Freese, and Gondolo proposed the idea of Dark Stars (DSs). Some of the first stars in the Universe might have been powered by Dark Matter (DM annihilations rather than nuclear fusion. They could form out of pristine Hydrogen and Helium clouds at the centers of protogalaxies, where there is a sufficient DM to serve as their heat source. They are very bright diffuse puffy objects and grow to be very massive. In 2023 three of us (C.I., J.P., and K.F.) identified the first three photometric DS candidates in the JWST NIRCam data. In this paper, we use JWST NIRSpec data and identify four spectroscopic DS candidates, one of them being the second most distant object ever observed.

The first stars to form in the Universe, when it was roughly 200 million years old (e.g., refs. 1–7), may have been Dark Stars (DSs), composed almost entirely of hydrogen and helium from the Big Bang but powered by Dark Matter (DM) annihilation rather than by nuclear fusion (8–10). Although DM constitutes only $\lesssim$0.1% of the stellar mass, this amount is sufficient to power a DS for millions to billions of years. The relevant types of DM for heating the stars include weakly interacting massive particles (WIMPs)* and self-interacting DM (SIDM) (11). Starting from their inception at $\sim$1 $M_\odot$, DSs accrete mass from their surroundings to become supermassive stars, some even reaching masses $\gtrsim 10^6 M_\odot$ and luminosities $\sim 10^9 L_\odot$, making them detectable with the James webb space telescope (JWST) (12–14) or the upcoming Roman space telescope (RST) (15). In ref. 16, three of us found several Super Massive DS (SMDS) candidates in the JADES of the JWST: JADES-GS-z11-0, JADES-GS-z12-0, and JADES-GS-z13-0. These objects are good fits to photometric NIRCam data predicted for SMDS using the TLUSTY (17) code for estimating spectral energy distributions (SEDs). One SMDS can be as bright as an entire early galaxy of stars. As shown by ref. 15, it is difficult, yet not impossible, to differentiate between isolated SMDSs and certain types of early galaxies based on spectroscopic or photometric data; spectroscopic data over a wide range of wavelengths (i.e., NIRSpec & ALMA) should help with this, as we will discuss.

The methodology of our current paper provides several improvements over our previous work (16): 1) we compute more accurate spectra and estimates of the size of SMDS (as would be seen by JWST); 2) we use recent spectroscopic data from NIRSpec (rather than the NIRCam photometry we used previously); and 3) we perform more careful statistical analyses in fitting the theoretical predictions to the data. Most interestingly, we find two new SDMS candidates in JWST data. Specifically, using publicly available NIRSpec data, we find that the measured spectra of two of the three previously identified photometric candidates (JADES-GS-z13-0 and JADES-GS-z11-0) are consistent with a DS interpretation (the third object we previously examined has some metal lines in it that imply it is not an isolated DS). Moreover, we identify two more spectroscopic DS candidates: JADES-GS-z14-1 and JADES-GS-z14-0, with the former being the second most distant spectroscopically confirmed object ever observed. Furthermore, we find a tentative ($S/N \sim 2$) He IIλ1640 absorption feature (a smoking gun for DSs) in the NIRSpec spectrum for JADES-GS-z14-0. As we were wrapping up this manuscript ref. 18 reported evidence of an O III nebular emission line in the

*This is the case for most previous works on DSs.

Author affiliations: [a]Department of Physics and Astronomy, Colgate University, Hamilton, NY 13346; [b]Department of Physics and Astronomy, University of Pennsylvania, Philadelphia, PA 19104-6396; [c]Weinberg Institute for Theoretical Physics, Texas Center for Cosmology and Astroparticle Physics, Department of Physics, University of Texas, Austin, TX 78712; [d]Department of Physics, Stockholm University, Stockholm SE-106 91, Sweden; and [e]Nordic Institute for Theoretical Physics, Stockholm SE-106 91, Sweden

Author contributions: C.I. and K.F. designed research; C.I., S.S.M., and J.P. performed research; S.S.M. and J.P. analyzed data; and C.I. and K.F. wrote the paper.

Reviewers: L.B., Universitat Zurich; and N.S., Stony Brook University.

The authors declare no competing interest.

[1]To whom correspondence may be addressed: cilie@colgate.edu or ktfreese@utexas.edu.

Published September 30, 2025.

ALMA measured spectrum of JADES-GS-z14-0. If both spectral features are confirmed, this object cannot be an isolated DS but rather may be a DS embedded in a metal rich environment as we plan to study in future work (*Discussion and Conclusion*).

Before proceeding, we wish to point out that the brightest and most massive SMDSs could resolve several conundrums of high redshift JWST data. First, JWST has discovered a larger than expected number of very bright high redshift objects (19–26). The high stellar masses inferred for the most luminous of these objects, if they are galaxies, requires an inexplicably high efficiency rate of conversion of gas to stellar material.[†] We argue that some of these overly massive and bright objects could instead be SMDSs.

In addition, SMDSs may provide an explanation of the many early Supermassive Black Holes (SMBHs) that are otherwise hard to explain. Once the SMDS runs out of DM fuel, it collapses to a black hole (BH), e.g., of $10^6 M_\odot$, thus providing excellent seeds for the even larger SMBHs found already at early times. JWST has found many such enormous SMBHs. BHs at $z \sim 6$ appear to be about three orders of magnitude more massive than what the local relation between BH and stellar masses would imply (32). The most striking such object is UHZ-1, an enormous SMBH at $z \sim 10$, with a mass of about ten billion suns. Emitting light when the universe was a mere 500 Myr old, UHZ-1 is considered to be the first indication of the need for very massive BH seeds (33). UHZ1 is just the tip of the iceberg when it comes $z \gtrsim 6$ quasars observed harboring SMBHs that are too big to have been seeded by regular stars (e.g., refs. 34–36). Even the most massive zero metallicity nuclear burning stars (i.e., $M \sim 10^3 M_\odot$)[‡] could have seeded such gigantic SMBHs only if they accreted for long periods of time at super Eddington rates. More likely, the data imply the need for heavy BH seeds, at high redshifts (33, 37). Direct collapse BHs (DCBHs) (e.g., refs. 35, 38–43) and DSs (e.g., refs. 8, 12, 44–46)[§] are two proposed mechanisms for producing such heavy BH seeds in the first few hundred million years after the Big Bang.

Thus DSs are a plausible solution to two of the most pressing puzzles in Astronomy today: i) the many brighter than expected high-z compact objects found by JWST and ii) the origin of the massive BH seeds required to explain many of the most distant quasars observed. We note that the case studied here is that of DSs powered solely by the DM passing through the central region of the halo (rather than additional DM that can be captured via elastic scattering with nuclei in the star, leading to hotter DSs). In this paper, for simplicity, we assume the DM is composed of 100 GeV WIMPs with a canonical annihilation cross section. In the future, we plan to examine a wider range of particle masses. In terms of the big picture, DSs do not look very different for WIMPs of masses ranging from GeVs to a few hundred TeVs (12, 47, 48); however, for lower WIMP masses, the heating rate is higher, so that the DSs are somewhat hotter. In a future study we plan to include the mass of the WIMP DM particle into the JWST data fitting pipeline developed here.

The rest of the paper is organized as follows: we begin by briefly discussing DSs and reviewing their main properties, we then proceed to explain our methodology of identifying spectroscopic DS candidates, followed by our *Results* and *Discussion and Conclusions*.

[†] Explanations have been put forward that alleviate this tension, e.g., due to top heavy Initial Mass Functions (e.g., refs. 27–30) or feedback free star burst formation episodes (31), to name a few.

[‡] For references on zero metallicity, a.k.a. Pop III, stars see, for example refs. 1–7.

[§] Note that DSs are sometimes called Pop III.1 stars in the literature (e.g., refs. 44–46).

DSs

In view of the lack of direct observations, numerical simulations are still the primary tool to describe the properties of the first stars (e.g., refs. 1–7), and galaxies (e.g., refs. 49–54) in the Universe. The first stars formed roughly 100 to 400 Myrs after the Big Bang ($z \sim 20$ to 10) as a consequence of the gravitational collapse of pristine, zero metallicity, molecular hydrogen clouds at the center of 10^6 to $10^8 M_\odot$ minihaloes. If the role of DM heating can be neglected during the collapse of the protostellar hydrogen clouds, the outcome is the formation of nuclear burning Population III stars. Those grow via mass accretion, reaching masses of (at most) $10^3 M_\odot$ (e.g., ref. 55), and populate the first small galaxies. However, as shown by ref. 8, if DM is formed of WIMPs, then DM heating inside a protostellar gas cloud at the center of high-z DM microhalos can be nonnegligible and it can even halt the gravitational collapse well before the central temperatures reach the critical values needed for nuclear fusion to begin. As such, a different type of first star can form: a DS (8, 9, 47).[¶]

Those exotic objects are made primarily of H and He, with DM accounting for less than 0.1% of their mass. Since DM annihilations are much more efficient at converting mass to energy than nuclear fusion, this small amount of DM can power the star, while maintaining a relatively cool core (i.e., $T_c \lesssim 10^7$ K). Those cool ($T_{eff} \lesssim 10^4$ K) puffy ($R_{DS} \sim 10$ AU) stars can accrete the surrounding baryons almost indefinitely, since the radiative feedback effects that shut off accretion in the case of Pop III stars are not significant for DSs (12). As such, they can grow to become supermassive (SMDSs), reaching masses $\sim 10^6 M_\odot$ and luminosities $\sim 10^{10} L_\odot$, making them visible to JWST (12, 14, 16) or Roman Space Telescope (RST) (15). In view of HST's sensitivity and the fact that no plausible DS candidates were identified with it, it is expected that isolated DSs very seldom survive past $z \lesssim 10$ (14).

Below we review some of the basic particle physics ingredients needed for the formation of DSs. We considered two types of DM particles: weakly interacting DM (WIMPs, in most papers) and self-interacting DM (SIDM) (11).[#] The energy production per unit volume provided by the annihilation of two DM particles is

$$Q = m_\chi n_\chi^2 \langle \sigma v \rangle = \langle \sigma v \rangle \rho_\chi^2 / m_\chi, \qquad [1]$$

where $m_\chi \sim 1\text{GeV} - 10\text{TeV}$ is the DM mass, n_χ is the DM number density, ρ_χ is the DM energy density. We assumed the standard annihilation cross section (the value that produces the correct DM abundance in the Universe today): $\langle \sigma v \rangle = 3 \times 10^{-26} \text{cm}^3/\text{s}$, although cross sections several orders of magnitude smaller or larger would work equally well since a decrease in $\langle \sigma v \rangle$ can be easily compensated by an increase in ρ_χ^2 / m_χ. The three conditions necessary for the formation of DSs are 1) sufficient DM density, 2) DM annihilation products become trapped inside the star, and 3) the DM heating rate beats the cooling rate of the collapsing cloud. Those are easily met for the case of WIMPs (8) and SIDM (11).

The high DM density condition can be met in one of two ways. As molecular clouds collapse inside high-z minihaloes, they pull in more DM as well. This is a purely gravitational effect, which leads to the significant enhancement of DM densities at the centers of said halos. Using adiabatic contraction (AC) (57)[‖] one can

[¶] For a review of DSs see ref. 56.

[#] As it turns out, for both WIMPs and SIDM the emerging DSs have very similar observable properties (11).

[‖] A formalism confirmed in more sophisticated analyses in the context of DSs in ref. 58.

estimate that the local DM densities where the first stars form can be as high as $\gtrsim 10^{14}$ GeVcm^{-3}. Since many DM particles are on chaotic or box orbits, the central DM density can be replenished and kept high for millions (to billions) of years. If or when this adiabatically contracted DM reservoir is depleted, the star begins to collapse. As a result it will reach sufficiently high baryonic densities, such that it is able to capture further DM particles from its vicinity via elastic scattering of the DM with the atoms in the star. DSs powered by Captured DM are somewhat hotter than those powered via AC, since they underwent a contraction phase. For simplicity, in this work, we only consider DSs powered by AC DM. Even with this restricting assumption, we find that all four objects analyzed are compelling DS candidates.

We use stellar structure solving codes to build up the mass of DSs from an initial value of $\sim 1 M_{\odot}$ via accretion to potentially very large masses. We simulate DS evolutionary tracks with two different types of stellar codes: one of which assumes that the DS can be approximated as polytrope of variable index (i.e., transitioning from 3/2 in the small mass stages, to 3 once the DS becomes fully radiation pressure dominated), and the MESA stellar evolution code (59). In both cases, we find essentially the same results (48). For simplicity, in this work, we only consider 100 GeV WIMPs powering DSs, and use the polytropic equilibrium models obtained in ref. 12. From the equilibrium structure we can derive observable properties and use those to identify candidates, as explained in detail in the next section.

In previous work, we obtained spectra for DSs using TLUSTY. We assumed that DSs could be treated as point sources in the data as they would be unresolved by JWST. However, in this paper, we make an important improvement. SEDs are refined using the CLOUDY code (60), which accounts for possible nebular emission generated by the ionization of surrounding hydrogen by Supermassive DSs. This effect has been first considered by ref. 61 for Supermassive DSs formed via DM Capture. For DSs formed via AC (such as those studied by us here), we find that the continuum spectra relevant to JWST remain largely unmodified, whereas nebular emission lines are present at wavelengths larger than observed in the JWST filters. However, DSs powering a nebula are no longer point sources and may be extended.

Methods

We use the most recent publicly available JWST advanced deep extragalactic survey (JADES) NIRSpec data in order to identify spectroscopic DS candidates. A first cut-off is imposed on the data, as follows: we select objects with confirmed spectroscopic redshift $z_{spec} \gtrsim 10$, which are either extremely compact or consistent with a point source, and for which no metal emission lines have been conclusively identified.** We specifically focus on the NIRSpec observations of JADES-GS-z11 and JADES-GS-z13, as described by Hainline et al. (63), and JADES-GS-z14-0 and JADES-GS-z14-1, as reported by Carniani et al. (64). These observations do not reveal any confident spectral lines with a signal-to-noise ratio exceeding 3 (within the JADES data; see below for remarks on ALMA data). As a result, we prioritize spectral fitting over the identification of individual spectral lines in our analysis.

For those objects that are consistent with a point source in the JWST data, (such as JADES-GS-z14-1 in this work), we model them as pure DSs without surrounding nebulae, i.e., we assume almost no gas left around them to be ionized. From the evolutionary tracks derived using polytropes in ref. 12 (see figure 1 and table 3 there) we extract relevant parameters (i.e., stellar mass, stellar radius, and surface temperature) needed to calculate the SED for DSs. We do so using TLUSTY (17, 65), and assume, as appropriate for DSs, zero metallicity stellar atmospheres and a primordial (i.e., Big Bang Nucleosynthesis) H and He abundance. It is important to note that fixing m_{χ} (as we did) leads to the restframe SED being dependent essentially only on one parameter, the stellar mass. As such, we have only two free parameters with which we model high-z point source objects as pure DSs: redshift (z) and stellar mass (M_{DS}) for which we find optimal values in order to fit the JADES spectral data.

We model the other three objects considered, which are compact but for which a half-radius (or angular size) is reported in the discovery papers, as DSs powering a spherical hydrogen nebula. Therefore, the pure DS SEDs are further refined using the CLOUDY code (60), which accounts for possible nebular emission generated by the ionization of surrounding hydrogen by Supermassive DSs. While DSs are not hot enough to turn off mass accretion via feedback effects, the most massive ones can power a nebula, as first shown by ref. 61. As such, for those objects we have three free parameters that determine observable spectra: redshift (z), stellar mass (M_{DS}), and the H density of the nebular cloud (n_H). Remarkably, we demonstrate that even with this minimal set of parameters, we can achieve compelling DS fits to all JADES galaxy candidates considered.

As default, we set the gravitational lensing factor to be $\mu = 1$ (no magnification). In ref. 16, we allowed μ to vary and found that our fits to data were always optimized for μ near 1. In this work, the only case with $\mu \neq 1$ is that of JADES-GS-z14-0, for which the discovery paper determined $\mu = 1.2$. We note here that the mass estimates for the DS models we will obtain here, could be easily rescaled if, in the future a value of $\mu \neq 1$ is determined for the three objects for which we assumed no magnification. Namely, $M_{SMDS}(\mu) \sim M_{SMDS}(\mu = 1)/\mu$. A lower mass DS would have a lower T which would shift the peak to a higher wavelength. However, $\mu \sim 1$ is the case for all the objects studied in this paper.

Spectral Fitting Technique. In order to fit our DS models to NIRSpec JADES data, we employ the Nelder–Mead algorithm (66), a robust optimization technique, to minimize the mean squared error between the simulated and observed spectral data. Observational uncertainties are incorporated through Monte Carlo simulations. For each point in the observed spectra, we define a range of values based on its upper and lower uncertainty bounds. A Gaussian probability distribution is generated for each spectral point, and we draw 100 random samples from these distributions. This approach allows us to perform 100 independent fits of the SED to the observed spectra, resulting in a range of parameter estimates rather than single-point predictions. Consequently, our analysis yields a comprehensive understanding of the likely values for the stellar mass, redshift, and where appropriate H density (n_H) of the nebula, while accounting for the uncertainties inherent in the observational data. In our MC runs we bias the value for the prior of n_H within a range that would lead to a Strömgren radius (i.e., radius of the HII nebular region surrounding the star) consistent with the reported physical size of the object itself. Our current approach is clearly superior to the simplistic χ^2 analysis we used in ref. 16 to identify DS candidates in JWST.

Radial Profile Fitting Technique. Three of the objects considered by us in this work (i.e., JADES-GS-z11-0, JADES-GS-z13-0, JADES-GS-z14-0) are extremely compact, with radii of at most a few hundred pc, whereas JADES-GS-z14-1 is consistent with a point source. We model the first three as DSs surrounded by a spherical hydrogen nebula. Their radial profiles are simulated using the JWST Exposure Time Calculator (ETC) Pandeia (67) and compared against radial profiles (in the standard F200W NIRCam band) reported in the literature (63, 64). We account for the uncertainties in the measured radial profiles via a Monte Carlo (MC) simulation, as explained below. The flux emitted by each object (which we input from our best fit DS spectral models described above), along with the angular size (a) of the object and the Sérsic index (n)†† are the three main ingredients needed to simulate radial profiles for our DSs surrounded by a nebula. For the flux, we use the best fit obtained via the procedure described above, whereas the other two are free parameters we fit for using our MC simulations. Specifically, for each case, a normal distribution is generated

** Note that in view of the results of ref. 62, who identify carbon nebular emission in JADES NIRSpec data for JADES-GS-z12-0, this object can no longer be considered as an isolated DS candidate. It could instead be a DS embedded within a Pop III/II galaxy, and we plan to test this hypothesis in future work.

†† The Sérsic profile (68) is a commonly assumed empirical law describing how the intensity falls with distance from the center of galaxies or star clusters. Namely, $I \sim \exp(-R^{1/n})$, with n being the Sérsic index.

for the observed radial profile points, using the reported uncertainties. We sample points from this distribution 75 times and find best fit for our two free parameters (*a* and *n*) using the standard Nedler-Mead optimization, which needs initial guesses for the free parameters. Since we assumed a spherical nebula, we bias the choice of our prior of the Sérsic index (*n*) to be sampled from a normal distribution centered around $n = 4$ (68). For *a*, our initial guess is informed by the value of the angular size for each object, as reported in refs. 63, 64. We find that our DS models have a radial profile that fits well the reported JWST data.

Results

Below we show that JADES-GS-z11-0, JADES-GS-z13-0, JADES-GS-z14-0, and JADES-GS-z14-1 can each be modeled by DSs, via the procedure described in our *Methods*.

Spectral Fits. In Figs. 1 and 2, we plot our best fit DS models (obtained according to the method described in the previous section) against JWST data (from refs. 63 and 64) for the four objects considered. Specifically, in Fig. 1, we plot our best fit Supermassive DS models against JWST JADES NIRSpec data for all four objects, whereas Fig. 2 (pg. 5) presents corner plots for the 2D and 1D marginalized posteriors for the free parameters of our SMDSs models.

The normalized residuals displayed at the bottom of each of the SEDs from Fig. 1 show that our Supermassive DS models lie consistently within $1-\sigma$ of the NIRSpec data for each of the four objects considered. Therefore, at the level the continuum of the emission flux they are each consistent with a DS interpretation (as shown here) and a galactic interpretation (63, 64). Probing higher wavelengths continuum with ALMA should, in principle, make the disambiguation between those two equally good interpretations possible. No conclusive emission lines are detected with NIRSpec for JADES-GS-z13-0, JADES-GS-z14-0[‡‡] or JADES-GS-z14-1,[§§] thus as of now, those objects are

[‡‡] ALMA follow-up observations for this object seem to favor the existence of an [O III]88μm emission line (18). We discuss this aspect further at the end of this section.

[§§] See also ref. 70, who, using NIRSpec/PRISM spectroscopy totaling 56 h reveals no rest-frame ultraviolet emission lines above 3σ.

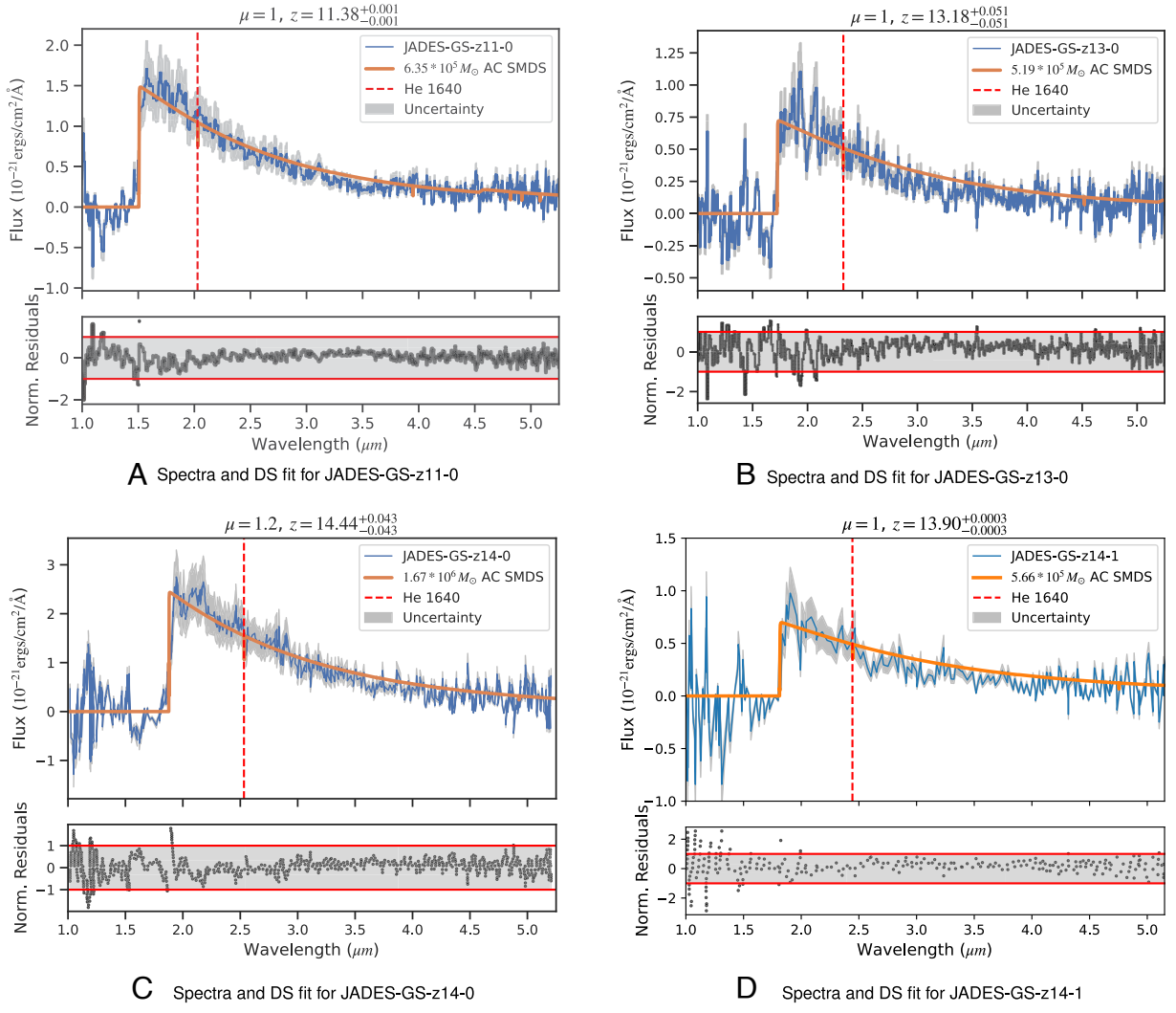

Fig. 1. (*A-D*) The first four Supermassive Dark Star spectral candidates. The data (blue line) and uncertainty band (shaded gray) plotted against our best fit DS models (orange line). The red dashed line represents where He IIλ1640 absorption feature, expected only for DSs, might be observed. The normalized residuals ($\frac{F_{simul} - F_{measured}}{\sigma_{measured}}$) displayed in the lower panels of each of the SEDs show that our Supermassive DS models lie consistently within $1-\sigma$ of the NIRSpec data for each of the four objects considered. The vertical drop in the fluxes represents the Lyman break, as expected for $z \gtrsim 6$ objects due to absorption by neutral H along the line of sight (69). The vast majority of the other "features" in the observed spectra are actually due to noise. In the title of each plot we display the values assumed for the gravitational lensing factor (μ) and the best fit values for z_{spec} (along with uncertainties).

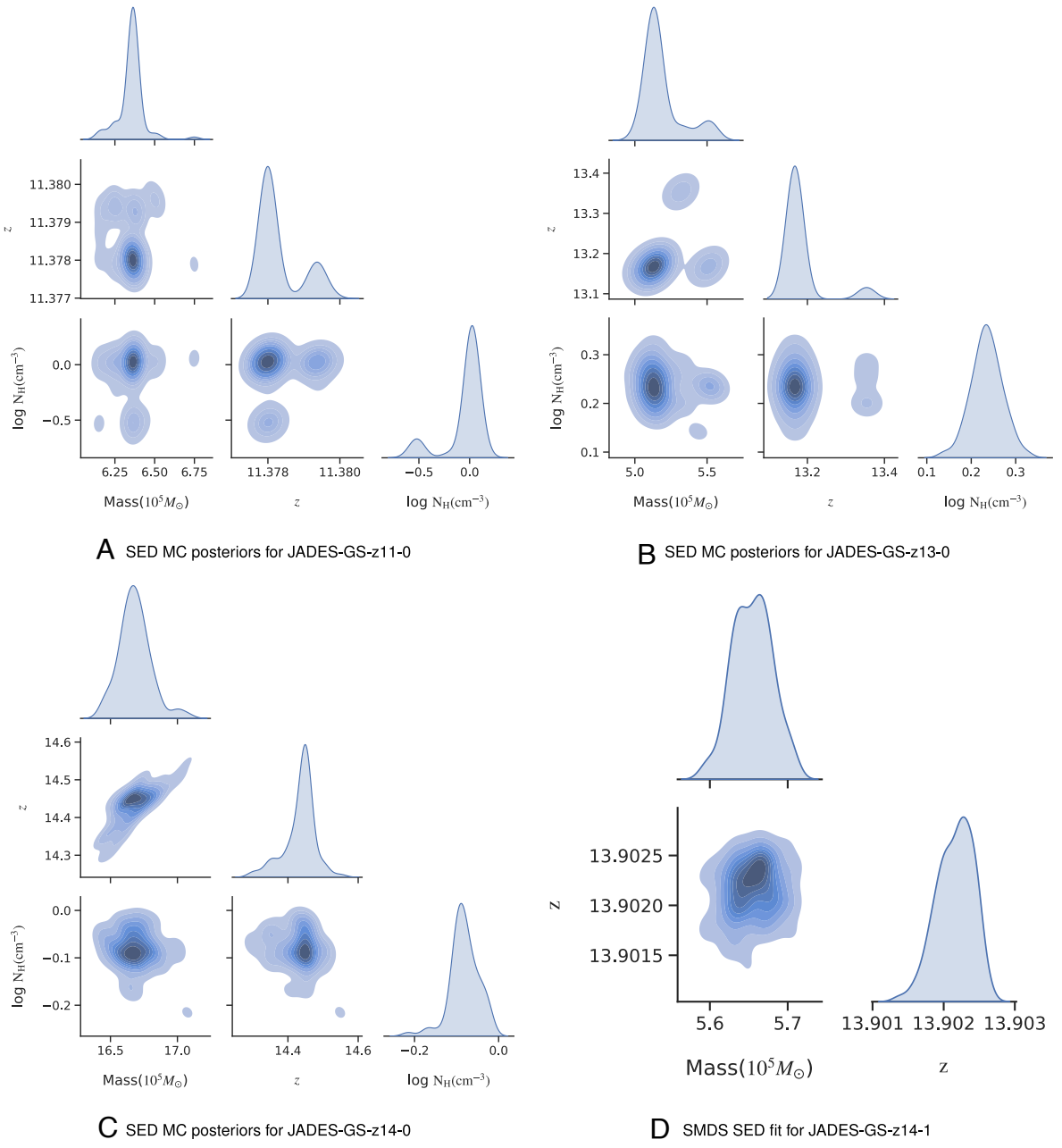

Fig. 2. (*A-D*) Corner plots representing 2D and 1D marginalized posteriors for the free parameters of our Supermassive DS spectral fits (as described in *Methods*). Note that for JADES-GS-z14-1 (lower right hand plot), since it is not resolved, we only need stellar mass (*M*) and redshift (*z*), whereas for the other three objects we include the number density of hydrogen (n_H) in the nebular cloud surrounding the DS. We assumed SMDSs are powered by 100 GeV WIMPs adiabatically contracted (AC) inside the star.

consistent with both a DS and a galaxy interpretation. Moreover, with deeper JWST spectra, any evidence of metal lines would rule out our simplistic model of an isolated SMDS (or a SMDS powering a zero metallicity nebula), whereas a detection of a He II λ1640 absorption feature would confirm the DS hypothesis. For JADES-GS-z11-0 NIRSpec PRISM data hints of three metal lines: the [O II]$\lambda\lambda$3726, 3729 doublet and the [N III]λ3869 (63). The higher-resolution NIRSpec G395M grating spectrum shows no evidence of the [O II]λ3726 part of the [O II] doublet, leading to an unphysically high [O II]λ3729 / [O II]λ3726 observed flux ratio (63). In view of this, and the relatively low SNR of the two remaining putative lines (i.e., $SNR = 2$ to 3) we consider JADES-GS-z11-0 a valid SMDSs candidate (see also Fig. 1*A*).

In Table 1 (pg. 6) we summarize the best fit parameters (including $1-\sigma$ uncertainties) of our Supermassive DS models for the four spectroscopic candidates identified in this work. One can see that the best fit mass for all of the candidates studied here is of order $\sim 10^6 M_\odot$.

Morphology Fits. JADES-GS-z14-1 is unresolved (64, 70). As such, its morphology matches that of a point source, such as an isolated Supermassive DS. As explained in our *Methods*, the other three JADES objects considered are compact, yet extended (63, 64). We model them as SMDSs powering a hydrogen ionization bound nebula, as described in detail in *Methods*. In Fig. 3 (pg. 6) we present our results of the MC

Table 1. Summary of SMDSs best fit parameters for the four spectroscopic candidates identified

Object name	Mass ($10^5\ M_\odot$)	Redshift (z)	$\log(N_H/cm^3)$
GS-z11	$6.35^{+0.08}_{-0.08}$	$11.38^{+0.001}_{-0.001}$	$-0.04^{+0.18}_{-0.18}$
GS-z13	$5.19^{+0.13}_{-0.13}$	$13.18^{+0.05}_{-0.05}$	$0.23^{+0.03}_{-0.03}$
GS-z14-0	$16.68^{+0.12}_{-0.12}$	$14.44^{+0.04}_{-0.04}$	$-0.1^{+0.03}_{-0.03}$
GS-z14-1	$5.65^{+0.02}_{-0.02}$	$13.90^{+0.0003}_{-0.0003}$	N/A

We use the short name for each object, i.e., we omit the JADES designation

Table 2. Summary of best fit morphological parameters

Object name	Angular size (arcsec)	Sérsic index
JADES-GS-z11-0	$0.10^{+0.04}_{-0.04}$	$4.00^{+0.05}_{-0.05}$
JADES-GS-z13-0	$0.066^{+0.0035}_{-0.0035}$	$4.00^{+0.03}_{-0.03}$
JADES-GS-z14-0	$0.27^{+0.01}_{-0.01}$	$3.99^{+0.04}_{-0.04}$

simulation for fitting the F200W radial profiles of JADES-GS-z11-0, JADES-GS-z13-0, and JADES-GS-z14-0 with the Supermassive DSs identified by the spectral fits already described. We restricted our analysis to a spherically symmetric nebula, and as such biased the Sérsic index to be sampled from a Gaussian distribution centered around $n = 4$. Even with this restrictive assumption, we find that the morphology of each of those three objects is consistent with our Supermassive DS models. In Table 2 (pg. 6) we summarize the values for our SMDS nebulae best fit parameters for the Sérsic index and angular size of each of the three resolved objects considered.

Spectral Features of DSs. Supermassive DSs have a distinct smoking gun signature: an absorption feature due to He II at 1640 Å. This is because the surface temperature of SMDSs leads to a significant number of singly ionized Helium (i.e. He II) atoms in the first excited state in their atmospheres (n=2); in turn, those are excellent absorbers of 1,640 Å photons (from $n = 2$ to $n = 3$ states). No other known high redshift objects are expected to produce such an absorption feature. Instead, early galaxies may have an emission feature at the same wavelength. Since the nuclear burning stars (with masses up to $\sim 500 M_\odot$) comprising these early galaxies have much hotter temperatures, they generate He III (fully ionized) regions in the nebulae surrounding them. Free electrons recombine with He III ions to form He II, and in the process emission at characteristic wavelengths is generated. The most prominent such feature is at 1,640 Å (i.e., $n = 3 \rightarrow 2$ in He II). As such, early galaxies dominated by massive and hot fusion powered stars exhibit strong H and He nebular emission lines, the most prominent being the Ly-α and the He IIλ1640 Thus, detection of the He IIλ1640 absorption feature would imply conclusive evidence for the existence of DSs. Further, their discovery could herald the first discovery of DM particles; follow-up studies could then elucidate the mass and interaction strength of the DM particles.

In Fig. 4, we show the identification of a He IIλ1640 absorption feature (S/N $\sim$ 2) in the NIRSpec observed flux of JADES-GS-z14-0. The spectroscopic redshift corresponding to this feature is $z \simeq 14.52$, which lies very close to the $2-\sigma$ confidence level of the best fit redshift we found in

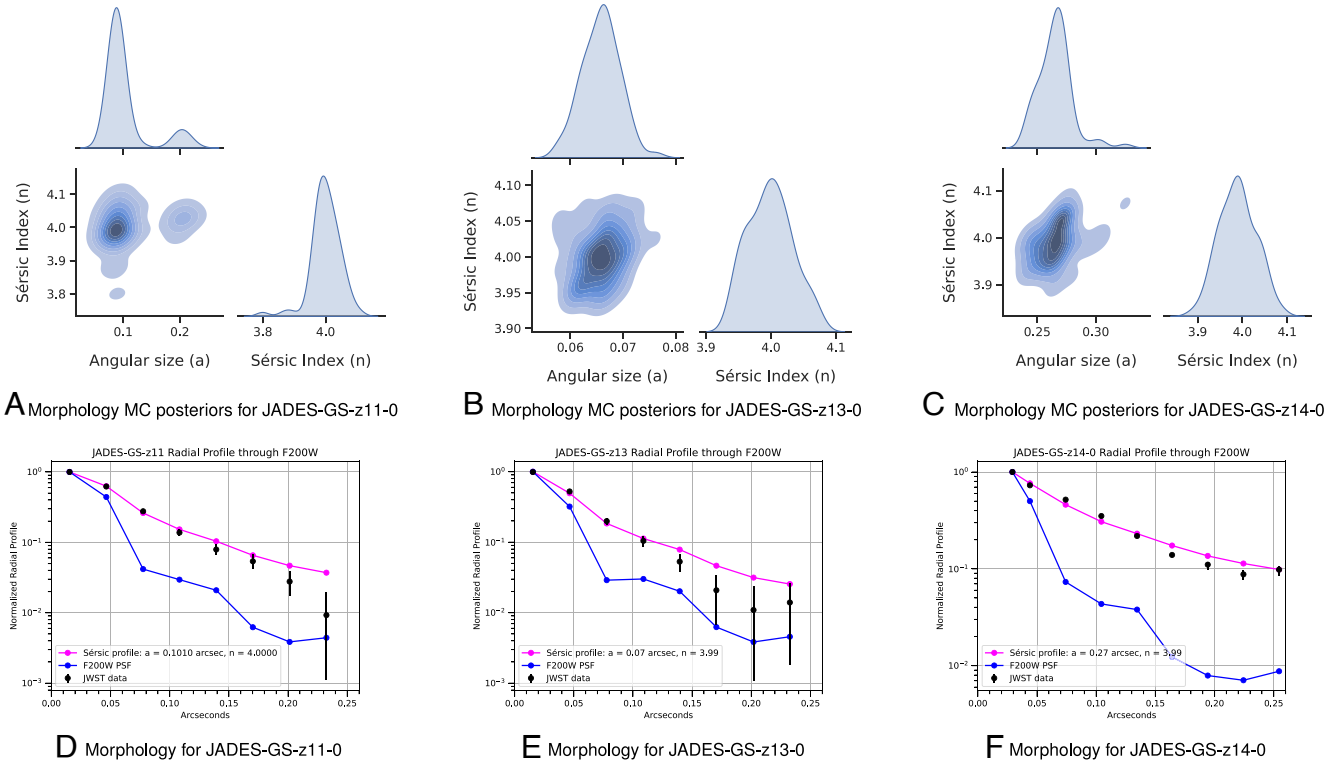

Fig. 3. *Top* panels (*A-C*): Corner plots representing 2D and 1D marginalized posteriors for the free parameters (Sérsic index and angular size in arcseconds) of our H ionization bound nebulae powered by Supermassive DS models for JADES-GS-z11-0, JADES-GS-z13-0, and JADES-GS-z14-0. For more details on the set up of the Monte Carlo simulation, see *Methods*. *Bottom* panels (*D-F*): Radial profiles though F200W NIRCam band for each object. Data are represented by black dots, whereas our best fit model is shown in red. The blue line (and dots) represent the Point Spread Function (PSF) for F200W.

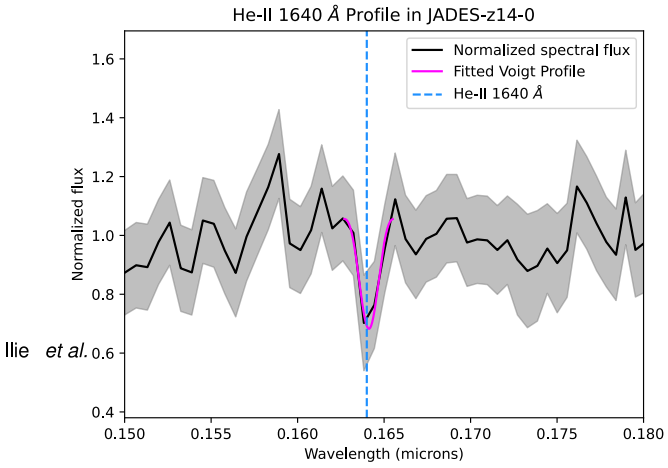

Fig. 4. Equivalent width of the potential He II absorption feature in JADES-GS-z14-0. The normalized spectral flux is plotted in black, the Voigt profile fit to the feature is in pink, and the line center is shown in the dashed blue line. The uncertainty in the flux is shown in gray. The equivalent width is calculated based on the Voigt profile fit and found to be 3.26 .

our global NIRSpec SED DS fit (Table 1).[¶] As such, this feature (if confirmed) is very likely the result of absorption of 1640 Åphotons by singly ionized He in the immediate vicinity of JADES-GS-z14-0. Sufficiently massive DSs have just the right temperature such that in their atmospheres this absorption process happens efficiently. We argue that the most plausible explanation would be a DS, as no other known astrophysical objects exhibit absorption at He IIλ1640. Moreover, the coincidence in the values of z_{spec} based on this feature, and the global SED fit makes the alternative explanation of absorption along the line of sight due to the presence of He II in the IGM highly improbable.

While encouraging and very exciting, we caution the reader not to interpret the feature identified by us in Fig. 4 as conclusive evidence for the existence of DSs. First and foremost, the Signal to Noise ratio is small (i.e., $S/N \sim 2$). Moreover, ref. 18 reports the discovery, with ALMA, of a [O III]88μm emission line ($S/N \sim 6$) in the spectrum of JADES-GS-z14-0, indicating a high level of metal enrichment in this system, not compatible with isolated DSs. At the end of *Discussion and Conclusion*, we discuss the implications of these spectral lines if confirmed in follow-up observations including the possibility of DSs in metal enriched environments.

Discussion and Conclusions

In this paper, we used publicly available NIRSpec JWST data for four high redshift spectroscopically confirmed objects previously found by the JADES in order to test the DS hypothesis. Three of those objects (JADES-GS-z11-0, JADES-GS-z13-0, and JADES-GS-z14-0) are compact, yet resolved with NIRCam. We modeled them as DSs powering a zero metallicity spherical nebula, with H and He in primordial abundance. JADES-GS-z14-1 is unresolved, and as such we model it as a pure supermassive DS. We find compelling DS fits for the observed spectra (Fig. 1) and morphology (Fig. 3) for each object analyzed.

Furthermore, for JADES-GS-z14-0, we identify a tentative He II λ1640 absorption feature (Fig. 4). As discussed above, caution is warranted when interpreting this potential feature as evidence for the DS hypothesis, especially in view of the relatively low S/N $\sim$ 2 and the very likely presence of a [O III]88μm emission line from this system (18). Only follow-up observation would conclusively rule out or confirm the DS hypothesis for this object, which is the first one for which we ever found evidence of a possible He II absorption feature. Both features (i.e., O III emission and He II absorption) surviving follow-up observations would be an extremely interesting scenario, as it would open up many questions. How could a DS find itself in such a metal rich environment? While we do not know the definitive answer to this important question yet, we foresee that it will not be specific to JADES-GS-z14-0 alone. For instance, in ref. 37, three of us showed that UHZ-1, a galaxy recently discovered by JWST at z $\sim$ 10, harboring a very bright quasar, could be evidence of a SMBH seeded by a DS, rather than a DCBH, e.g., as cited by Bogdán et al. (33). In our paper on UHZ1, we showed that there are two plausible ways for DSs to be embedded in a low metallicity galaxy: i) Mergers and ii) Same DM halo host. In the first scenario the DS forms in isolation, and its host halo merges with a DM halo hosting a metal enriched stellar population, whereas in the second scenario, we show that DSs and Pop III stars could, in principle, have formed almost simultaneously in the same host halo from pristine molecular clouds. The subsequent evolution of the most massive Pop III stars would lead to metal enrichment. As such, it is entirely plausible that a DS could find itself in a low metallicity environment, where a significant fraction of the light is emitted by nuclear burning stars. Motivated by our findings here and in ref. 37, we plan to investigate this aspect in more depth in the near future, and generate spectral templates in order to look for evidence of existence of such hybrid systems.

Another planned improvement on our DS interpretation of the JWST data will be to go beyond the particular choice of 100 GeV WIMP DM assumed in this paper, and instead take the mass of the DM particle as a free parameter for our fits. In previous work, we showed that the basic picture of DS formation remains unchanged for a variety of masses, but lighter WIMPs deposit more heat and therefore the resulting DS are somewhat hotter. In future work, we will use MESA to generate DSs powered by WIMPs of various masses, and generate TLUSTY/CLOUDY SED templates which will then be incorporated in our expanded MC fitting routines. Once a sufficiently large sample of DS candidates is identified, this would allow us to estimate the most likely values the DM particle mass and its annihilation cross section. In turn, this could inform direct detection experiments which regions of parameter space to target.

Data, Materials, and Software Availability. This work is based, in part, on observations made with the NASA/ESA/CSA James Webb Space Telescope. The data were obtained from the Mikulski Archive (71) for Space Telescopes at the Space Telescope Science Institute, which is operated by the Association of Universities for Research in Astronomy, Inc., under NASA contract NAS 5-03127 for JWST. These observations are associated with programs 1210, 1287, 3215, and the reduced data we used here is described in detail in (63, 64). The codes used to analyze the data can be shared upon request via email to either of the corresponding author(s).

ACKNOWLEDGMENTS. C.I. acknowledges funding from Colgate University via the Research Council (Grant No. 821028) and the Picker Interdisciplinary Science Institute (Grant No. 826837). K.F. is grateful for support from the Jeff & Gail Kodosky Endowed Chair in Physics at the University of

[¶] We furthermore performed a separate MC parameter fit, where we fixed $z = 14.52$ and let only the DS mass and n_H run. This new fit shows results consistent with our previous runs, as neither the stellar mass nor n_H change appreciably.

Texas at Austin. K.F. also acknowledges funding from the US Department of Energy under Grant DE-SC-0022021, as well as the Swedish Research Council (Contract No. 638-2013-8993). J.P. thanks the LSST-DA Data Science Fellowship Program, which is funded by LSST-DA, the Brinson Foundation, the WoodNext Foundation, and the Research Corporation for Science Advancement Foundation; her participation in the program has benefited this work. C.I. and S.S.M. acknowledge the use of Colgate's Turing Supercomputer (Partially supported by NSF grant OAC-2346664). We also thank Facundo Pérez Paolino for discussions regarding our S/N analysis of the He II feature identified.

1. T. Abel, G. L. Bryan, M. L. Norman, The formation of the first star in the Universe. *Science* **295**, 93 (2002).
2. R. Barkana, A. Loeb, In the beginning: The First sources of light and the reionization of the Universe. *Phys. Rep.* **349**, 125–238 (2001).
3. V. Bromm, R. B. Larson, The First stars. *Annu. Rev. Astron. Astrophys.* **42**, 79–118 (2004).
4. N. Yoshida, K. Omukai, L. Hernquist, T. Abel, Formation of primordial stars in a lambda-CDM universe. *Astrophys. J.* **652**, 6–25 (2006).
5. B. W. O'Shea, M. L. Norman, Population III star formation in a lambda-CDM Universe. 1. The effect of formation redshift and environment on protostellar accretion rate. *Astrophys. J.* **654**, 66–92 (2007).
6. N. Yoshida, K. Omukai, L. Hernquist, Protostar formation in the early universe. *Science* **321**, 669 (2008).
7. V. Bromm, N. Yoshida, L. Hernquist, C. F. McKee, The formation of the first stars and galaxies. *Nature* **459**, 49–54 (2009).
8. D. Spolyar, K. Freese, P. Gondolo, Dark matter and the first stars: A new phase of stellar evolution. *Phys. Rev. Lett.* **100**, 051101 (2008).
9. K. Freese, P. Bodenheimer, D. Spolyar, P. Gondolo, Stellar structure of Dark Stars: A first phase of Stellar evolution due to Dark Matter annihilation. *Astrophys. J.* **685**, L101–L112 (2008).
10. F. Iocco *et al.*, Dark matter annihilation effects on the first stars. *Mon. Not. R. Astron. Soc.* **390**, 1655–1669 (2008).
11. Y. Wu, S. Baum, K. Freese, L. Visinelli, H. B. Yu, Dark Stars powered by self-interacting Dark Matter. *Phys. Rev. D* **106**, 043028 (2022).
12. K. Freese, C. Ilie, D. Spolyar, M. Valluri, P. Bodenheimer, Supermassive Dark Stars: Detectable in JWST. *Astrophys. J.* **716**, 1397–1407 (2010).
13. E. Zackrisson *et al.*, Finding high-redshift Dark Stars with the James Webb space telescope. *Astrophys. J.* **717**, 257–267 (2010).
14. C. Ilie, K. Freese, M. Valluri, I. T. Iliev, P. R. Shapiro, Observing supermassive dark stars with James Webb space telescope. *Mon. Not. R. Astron. Soc.* **422**, 2164–2186 (2012).
15. S. Zhang, C. Ilie, K. Freese, Detectability of supermassive dark stars with the Roman space telescope. *Astrophys. J.* **965**, 121 (2024).
16. C. Ilie, J. Paulin, K. Freese, Supermassive Dark Star candidates seen by JWST. *Proc. Nat. Acad. Sci. U.S.A.* **120**, e2305762120 (2023).
17. I. Hubeny, T. Lanz, Tlusty user's guide. III: Operational manual. arXiv [Preprint] (2017). https://arxiv.org/abs/1706.01937 (Accessed 6 July 2025).
18. S. Carniani *et al.*, The eventful life of a luminous galaxy at z= 14: Metal enrichment, feedback, and low gas fraction?. *Astron. Astrophys.* **696**, A87 (2025).
19. R. P. Naidu *et al.*, Two remarkably luminous galaxy candidates at $z \approx 11 - 13$ revealed by JWST. *ApJL* **940**, 11 (2022).
20. S. L. Finkelstein *et al.*, A long time ago in a galaxy far, far away: A candidate z 14 galaxy in early JWST CEERS imaging. *ApJL* **940**, L55 (2022).
21. C. T. Donnan *et al.*, The evolution of the galaxy UV luminosity function at redshifts z 8–15 from deep JWST and ground-based near-infrared imaging. *Mon. Not. R. Astron. Soc.* **518**, 6011–6040 (2022).
22. R. P. Naidu *et al.*, Schrodinger's galaxy candidate: Puzzlingly luminous at $z \approx 17$, or dusty/quenched at $z \approx 5$? arXiv [Preprint] (2022). https://arxiv.org/abs/2208.02794 (Accessed 1 July 2025).
23. B. E. Robertson *et al.*, Discovery and properties of the earliest galaxies with confirmed distances. *Nat. Astron.* **7**, 611–621 (2023).
24. E. Curtis-Lake *et al.*, Spectroscopic confirmation of four metal-poor galaxies at z=10.3–13.2. *Nat. Astron.* **7**, 622-632 (2023).
25. I. Labbe *et al.*, A population of red candidate massive galaxies 600 Myr after the Big Bang. *Nature* **616**, 266–269 (2023).
26. M. Xiao *et al.*, Accelerated formation of ultra-massive galaxies in the first billion years. *Nature* **635**, 311–315 (2024).
27. S. L. Finkelstein *et al.*, CEERS key paper. I. An early look into the first 500 Myr of galaxy formation with JWST. *Astrophys. J. Lett.* **946**, L13 (2023).
28. Y. Harikane *et al.*, Pure spectroscopic constraints on UV luminosity functions and cosmic star formation history from 25 galaxies at $z_{\rm spec} = 8.61 - 13.20$ confirmed with JWST/NIRSPEC. *Astrophys. J.* **960**, 22 (2023).
29. L. Y. A. Yung, R. S. Somerville, S. L. Finkelstein, S. M. Wilkins, J. P. Gardner, Are the ultra-high-redshift galaxies at $z \geq 10$ surprising in the context of standard galaxy formation models? *Mon. Not. R. Astron. Soc.* **527**, 5929–5948 (2023).
30. J. J. Ziegler, K. Freese, J. Lozano, G. Montefalcone, Explaining the "too massive" high-redshift galaxies in JWST data: Numerical study of three effects and a simple relation. arXiv [Preprint] (2025). https://arxiv.org/abs/2507.21409 (Accessed 20 July 2025).
31. A. Dekel, K. C. Sarkar, Y. Birnboim, N. Mandelker, Z. Li, Efficient formation of massive galaxies at cosmic dawn by feedback-free starbursts. *Mon. Not. R. Astron. Soc.* **523**, 3201–3218 (2023).
32. I. Juodžbalis *et al.*, A dormant overmassive black hole in the early universe. *Nature* **636**, 594–597 (2024).
33. Á. Bogdán *et al.*, Evidence for heavy-seed origin of early supermassive black holes from a $z \approx 10$ X-ray quasar. *Nat. Astron.* **8**, 126–133 (2024).
34. F. Wang *et al.*, Exploring reionization-era quasars. III. Discovery of 16 quasars at $6.4 \lesssim z \lesssim 6.9$ with DESI legacy imaging surveys and the UKIRT hemisphere survey and quasar luminosity function at z *sim* 6.7. *Astrophys. J.* **884**, 30 (2019).
35. K. Inayoshi, E. Visbal, Z. Haiman, The assembly of the first massive black holes. *Annu. Rev. Astron. Astrophys.* **58**, 27–97 (2020).
36. A. Lupi, Z. Haiman, M. Volonteri, Forming massive seed black holes in high-redshift quasar host progenitors. *Mon. Not. R. Astron. Soc.* **503**, 5046–5060 (2021).
37. C. Ilie, K. Freese, A. Petric, J. Paulin, Uhz1 and the other three most distant quasars observed: Possible evidence for supermassive dark stars. arXiv [Preprint] (2023). https://arxiv.org/abs/2312.13837 (Accessed 2 July 2025).
38. A. Loeb, F. A. Rasio, Collapse of primordial gas clouds and the formation of quasar black holes. *Astrophys. J.* **432**, 52 (1994).
39. M. C. Begelman, M. Volonteri, M. J. Rees, Formation of supermassive black holes by direct collapse in pre-galactic haloes. *Mon. Not. R. Astron. Soc.* **370**, 289–298 (2006).
40. G. Lodato, P. Natarajan, Supermassive black hole formation during the assembly of pre-galactic discs. *Mon. Not. R. Astron. Soc.* **371**, 1813–1823 (2006).
41. P. Natarajan *et al.*, Mapping substructure in the HST Frontier Fields cluster lenses and in cosmological simulations. *Mon. Not. R. Astron. Soc.* **468**, 1962–1980 (2017).
42. K. S. S. Barrow, A. Aykutalp, J. H. Wise, Observational signatures of massive black hole formation in the early universe. *Nat. Astron.* **2**, 987–994 (2018).
43. D. J. Whalen *et al.*, Finding direct-collapse black holes at birth. *Astrophys. J. Lett.* **897**, L16 (2020).
44. N. Banik, J. C. Tan, P. Monaco, The formation of supermassive black holes from Population III.1 Seeds. I. Cosmic formation histories and clustering properties. *Mon. Not. R. Astron. Soc.* **483**, 3592–3606 (2019).
45. J. Singh, P. Monaco, J. C. Tan, The formation of supermassive black holes from population III.1 Seeds. II. Evolution to the local universe. *Mon. Not. R. Astron. Soc.* **525**, 969–982 (2023).
46. V. Cammelli *et al.*, The formation of supermassive black holes from population III.1 Seeds. III. Galaxy evolution and black hole growth from semi-analytic modelling. *Mon. Not. R. Astron. Soc.* **536**, 851–870 (2025).
47. D. Spolyar, P. Bodenheimer, K. Freese, P. Gondolo, Dark Stars: A new look at the First Stars in the Universe. *Astrophys. J.* **705**, 1031–1042 (2009).
48. T. Rindler-Daller, M. H. Montgomery, K. Freese, D. E. Winget, B. Paxton, Dark Stars: Improved models and first pulsation results. *Astrophys. J.* **799**, 210 (2015).
49. A. Loeb, *How Did the First Stars and Galaxies Form?* (Princeton University Press, Princeton, NJ, 2010).
50. V. Bromm, N. Yoshida, The first galaxies. *Annu. Rev. Astron. Astrophys.* **49**, 373–407 (2011).
51. N. Y. Gnedin, Cosmic reionization on computers: The faint end of the galaxy luminosity function. *Astrophys. J. Lett.* **825**, L17 (2016).
52. P. Dayal, A. Ferrara, Early galaxy formation and its large-scale effects. *Phys. Rep.* **780**, 1–64 (2018).
53. L. A. Yung, R. S. Somerville, S. L. Finkelstein, G. Popping, R. Davé, Semi-analytic forecasts for JWST-I. UV luminosity functions at z= 4–10. *Mon. Not. R. Astron. Soc.* **483**, 2983–3006 (2019).
54. P. Behroozi *et al.*, The universe at $z \geq 10$: Predictions for JWST from the UniverseMachine DR1. *Mon. Not. R. Astron. Soc.* **499**, 5702–5718 (2020).
55. S. Hirano *et al.*, One hundred first stars: Protostellar evolution and the final masses. *Astrophys. J.* **781**, 60 (2014).
56. K. Freese, T. Rindler-Daller, D. Spolyar, M. Valluri, Dark stars: A review. *Rep. Progr. Phys.* **79**, 066902 (2016).
57. G. R. Blumenthal, S. Faber, R. Flores, J. R. Primack, Contraction of dark matter galactic halos due to baryonic infall. *Astrophys. J.* **301**, 27–34 (1986).
58. K. Freese, P. Gondolo, J. Sellwood, D. Spolyar, Dark Matter densities during the formation of the first stars and in Dark Stars. *Astrophys. J.* **693**, 1563–1569 (2009).
59. B. Paxton *et al.*, Modules for experiments in stellar astrophysics (MESA). *Astrophys. J.* **192**, 3 (2011).
60. M. Chatzikos *et al.*, The 2023 release of cloudy. *Rev. Mex. Astron. Astrofis* **59**, 327-343 (2023).
61. E. Zackrisson, The observational signatures of high-redshift dark stars. arXiv [Preprint] (2011). https://arxiv.org/abs/1101.2895 (Accessed 2 July 2025).
62. F. d'Eugenio *et al.*, Jades: Carbon enrichment 350 Myr after the Big Bang. *Astron. Astrophys.* **689**, A152 (2024).
63. K. N. Hainline *et al.*, Searching for emission lines at $z \geq 11$: The role of damped lyα and hints about the escape of ionizing photons. *Astrophys. J.* **976**, 160 (2024).
64. S. Carniani *et al.*, Spectroscopic confirmation of two luminous galaxies at a redshift of 14. *Nature* **633**, 318–322 (2024).
65. I. Hubeny, A computer program for calculating non-LTE model stellar atmospheres. *Comput. Phys. Commun.* **52**, 103–132 (1988).
66. S. Singer, J. Nelder, Nelder–Mead algorithm. *Scholarpedia* **4**, 2928 (2009).
67. T. E. Pickering *et al.*, "Pandeia: A multi-mission exposure time calculator for JWST and WFIRST" in *Observatory Operations: Strategies, Processes, and Systems VI*, A. B. Peck, C. R. Benn, R. L. Seaman. Eds. (SPIE, 2016).
68. J. L. Sersic, *Atlas de Galaxias Australes* (Cordoba, Argentina: Observatorio Astronomico, 1968).
69. J. E. Gunn, B. A. Peterson, On the density of neutral hydrogen in intergalactic space. *Astrophys. J.* **142**, 1633–1636 (1965).
70. Z. Wu *et al.*, Jades-gs-z14-1: A compact, faint galaxy at $z \approx 14$ with weak metal lines from extremely deep JWST MIRI, NIRCAM, and NIRSPEC observations. arXiv [Preprint] (2025). https://arxiv.org/abs/2507.22858 (Accessed 5 August 2025).
71. STScI, Mast: Barbara A. Mikulski Archive for Space Telescopes. Mikulski Archive. https://mast.stsci.edu/portal/Mashup/Clients/Mast/Portal.html. Accessed 7 February 2025.